

Observation of a Constant Average Angular Momentum for Fusion at Sub-Barrier Energies

R. G. Stokstad, D. E. DiGregorio,^(a) K. T. Lesko, B. A. Harmon, E. B. Norman,
J. Pouliot, and Y. D. Chan

Nuclear Science Division, Lawrence Berkeley Laboratory, 1 Cyclotron Road, Berkeley, California 94720

(Received 6 September 1988)

The cross sections for the fusion reaction $^{128}\text{Te}(^{12}\text{C}, 3n)^{137}\text{Ce}$ were measured from $E_{\text{c.m.}} = 34.5$ to 50 MeV by observing the decay of the ground ($J^\pi = \frac{3}{2}^+$, $t_{1/2} = 9.0$ h) and isomeric ($\frac{11}{2}^-$, 34.4 h) states in ^{137}Ce . The isomer ratio decreases rapidly from a value of ≈ 34 at 47 MeV to an essentially constant value of ≈ 1.5 below 38 MeV. This confirms the prediction of an approximately constant value for the average angular momentum for fusion of heavy ions at energies well below the fusion barrier.

PACS numbers: 25.70.Jj

Measurements of fusion cross sections at energies near and below the fusion barrier have shown how the coupling of the entrance channel to structural and dynamical degrees of freedom (deformation, vibration, and nucleon transfer, for example) enhances the fusion cross section.^{1,2} The deduction of the moments of the distribution of angular momenta leading to fusion through the measurement of γ -ray multiplicity or fission angular correlations has provided important additional information on the fusion process.³⁻⁶

Dasso and Landowne⁷ have pointed out an interesting consequence of the quantum-mechanical nature of barrier penetration for the distribution of partial-wave cross sections σ_l . While the distribution shifts rapidly to lower values of l as the bombarding energy is decreased through the barrier region, the shape of the distribution is predicted to become constant at and below some bombarding energy $E_s = V_b - F$. Here, V_b is the fusion barrier and F is a measure of the strength of the coupling to other channels. While E_s thus depends on the barrier height and the coupling, the limiting shape of the distribution does not. In particular, the average angular momentum \bar{l} is given by

$$\bar{l} = \frac{4}{3} (\mu R_b^2 \epsilon / \hbar^2)^{1/2}, \quad (1)$$

where μ is the reduced mass, R_b is the radius corresponding to the top of the barrier, and ϵ is related to the curvature of the barrier and is given by

$$\epsilon = \frac{\hbar}{2\pi} \left[-\frac{1}{\mu} \frac{\partial^2 V(R_b)}{\partial r^2} \right]^{1/2}. \quad (2)$$

(Only in the limit of an infinitely thick barrier, for which $\epsilon \rightarrow 0$, would the cross section for heavy-ion fusion proceed solely by s -wave capture.) Nolan *et al.*⁸ have also noted that σ_l is predicted to be independent of E at energies below the barrier. The derivation of Eq. (1) is based on the Hill-Wheeler inverted-parabola approximation for the Coulomb-plus-nuclear potential. It neglects the change in the *shape* of the barrier caused by the centrifugal potential and the $1/r$ dependence of the Coulomb

potential at large values of r . Numerical calculations that treat the barrier penetration problem for the combined nuclear, Coulomb, and centrifugal potentials without these approximations indicate that \bar{l} is given approximately by Eq. (1) but that \bar{l} decreases slowly with energy below E_s . However, a marked decrease in the *slope* of \bar{l} near E_s is a general feature of all predictions, and is associated with the onset of an exponential behavior of the penetrability at lower bombarding energies.⁹ Given the general nature of this prediction, it is important to test it by experiment.

We report in this Letter the first observation of this behavior of the average angular momentum at energies well below the barrier. We also find that the predicted value of \bar{l} is consistent with experiment for the sub-barrier fusion of ^{12}C with ^{128}Te .

We have selected an experimental technique that is different than those mentioned above and used recently in the study of angular momentum in sub-barrier fusion reactions. Its features are ideally suited to this particular problem. By measuring the ratio R of the cross section for population of a high-spin isomeric state to that of a low-spin ground state, we obtain a measure of the distribution of angular momentum in the entrance channel^{10,11} while, at the same time, through the observation of delayed x rays, we are able to measure the small cross sections at which the effect is predicted to occur. The ground and isomeric states in ^{37}Ce (see Fig. 1) were populated by the reaction $^{128}\text{Te}(^{12}\text{C}, 3n)$ with use of the beam from the LBL 88-In. cyclotron. Targets were made by the evaporation of metallic tellurium (150–200 $\mu\text{g}/\text{cm}^2$, 98.7% ^{128}Te) onto catcher foils of carbon and gold, and were then arranged in a stack to permit data collection at several energies in a single irradiation. Additional foils could be inserted after a catcher foil to further reduce the beam energy for the next target.

After a bombardment of typically 8 h at intensities of ≤ 250 nA (electric), the x and γ radiation from the target-catcher foils were counted off-line for several days. Several $\approx 110\text{-cm}^3$ high-purity germanium detectors were used to collect 2048 or 4096 channel spectra in

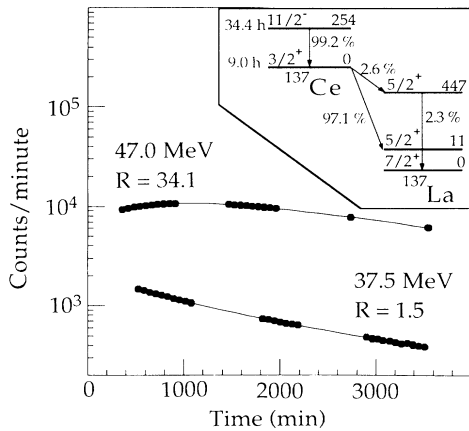


FIG. 1. The time dependence of the summed Ce and La K x rays obtained at $E_{c.m.} = 37.5$ and 47 MeV. The curves are fits with the data and result in the indicated values for the isomer ratio.

1-h time bins. Data were accumulated and recorded for subsequent analysis on an IBM PC/AT computer. Post irradiation measurements of the tellurium targets using proton-induced x-ray emission gave precise values for the thicknesses and also verified that there was no loss of target material during the bombardment. Checks that all the activity entered and was retained in the catcher-degrader foils were also made. The average energy loss and straggling for projectiles passing through the stack was measured by detecting beam particles with a silicon detector at 0°, with and without the stack. The measured energy loss agreed well with that calculated from tabulated stopping powers and the measured foil thicknesses. The absolute fusion cross sections and isomer ratios were determined by fitting the time dependence of the x-ray radioactivity following the bombardment.¹² The characteristic decay curves for a small and a large isomer ratio are shown in Fig. 1.

The cross sections for producing ¹³⁷Ce and the associated isomer ratios are shown in Fig. 2. These cross sections do not agree with those reported twenty years ago by Kiefer and Street.¹¹ While the isomer ratios agree fairly well at the lowest energies studied by these authors, our values become systematically larger with increasing bombarding energy. These discrepancies may have their origins in Kiefer's and Street's use of NaI detectors (with their relatively poor energy resolution) and in imprecisely known beam energies.

Note that R decreases rapidly and is then approximately constant for energies below 38 MeV. The approximate constancy of R indicates that the cross sections for fusion proceeding through partial waves (i) above, and (ii) below some critical value also have a constant, energy independent ratio. With the assumption that the individual partial-wave cross sections vary smoothly with energy, this result implies a constant aver-

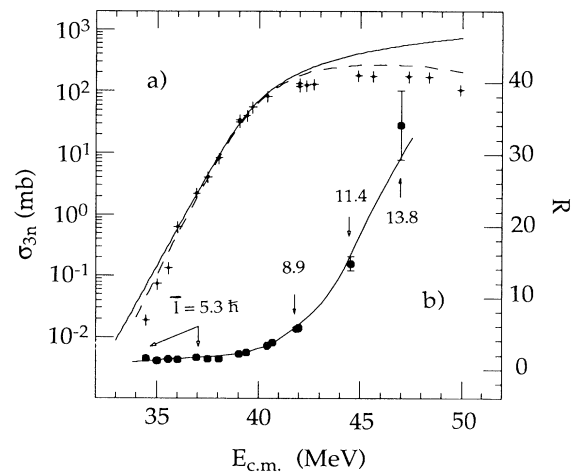


FIG. 2. (a) The experimental cross sections for the reaction $^{128}\text{Te}(^{12}\text{C}, 3n)^{137}\text{Ce}$. The vertical error bars include statistical and systematic errors. The horizontal bars represent the difference in the beam energy at the entrance and exit of the target combined with an estimate of the variation in beam energy due to straggling. The full curve is a calculation of the total fusion cross section as described in the text. The dashed curve shows the prediction for the 3n cross section, obtained with use of the predicted xn distributions. (b) The experimental isomer ratio. The vertical error bars are standard deviations. The full curve is a prediction based on the angular momentum distribution predicted by CCFUS and a statistical-decay calculation made with the code PACE. The predicted average angular momentum is indicated for selected bombarding energies.

age angular momentum for fusion. This conclusion is based on our general knowledge of the role of angular momentum in the neutron and γ -ray decay of compound nuclei, and not on the details of a particular statistical-model calculation.

It is possible to be more quantitative by making a detailed examination of the relationship of the isomer ratio to the angular momentum distribution in the ¹⁴⁰Ce compound nucleus and the subsequent changes caused by the evaporation of three neutrons and the γ rays preceding the population of the ground state or isomer. The partial-wave cross sections were calculated with the simplified coupled-channels computer code CCFUS of Dasso and Landowne,¹³ which employs the parabolic-barrier approximation. Known electromagnetic coupling matrix elements in the projectile and target nuclei were included, and the parameters describing the nuclear-plus-Coulomb potential ($V_b = 39.8$ MeV, $R_b = 10.57$ fm, $\epsilon = 0.7$ MeV) were obtained by scaling the values determined experimentally for ¹⁶O+Sm.¹⁴ The statistical decay of the compound nucleus was calculated with use of the computer code PACE,¹⁵ which included $E1$ and $E2$ γ -ray decay in competition with neutron emission. The input parameters used in this calculation were taken

from Ref. 16 and are those that reproduce the measured xn distributions for the fusion of ^{16}O with the isotopes of Sm.^{16,17} Known states in ^{137}Ce below 2 MeV having spins of $\frac{1}{2}$, $\frac{3}{2}$, and $\frac{5}{2}$, as well as the band built on the isomeric level were included in the calculation.¹⁸ Since states having spins of $\frac{7}{2}$ and $\frac{9}{2}$ must also be present below 2 MeV, they were inserted in the level scheme at random energies according to an estimated density. Above 2 MeV, the rigid-body moments of inertia calculated by Sierk,¹⁹ and the level-density formula of Gilbert and Cameron²⁰ were used. The results of these calculations indicate that the $3n$ channel exhausts $\geq 80\%$ of the fusion cross section between $E_{c.m.} = 36$ and 43 MeV, which covers most of the region of interest.

The predicted total fusion cross sections and those for the $3n$ channel alone are shown in Fig. 2. These predictions agree well with the experimental data from the barrier energy down to about 35 MeV. (Comparison with numerical calculations suggests that the steeper slope of the experimental data at the very lowest energies represents the breakdown of the parabolic approximation for the barrier.) However, this calculation does overestimate the $3n$ experimental cross section for $^{12}\text{C} + ^{128}\text{Te}$ in the above-barrier region. To check this we have also made a similar calculation for the $^{16}\text{O} + \text{Sn}$ total fusion cross sections, which have been measured by Jacobs *et al.*,²¹ and also find an overestimate. This leads us to conclude that the theoretical value for the total cross section is high rather than the statistical-model calculation of the $3n$ -to-total ratio being too low.

The isomer ratios predicted by the same calculation are compared to the experimental results also in Fig. 2. The values of \bar{l} in the entrance channel are indicated. The agreement is very good and shows that the prediction of an approximately constant angular momentum distribution at low energies is quantitatively consistent with the experimental data. The effects of angular momentum fractionation, i.e., the different xn channels being populated by different distributions, are automatically taken into account by the statistical-model calculation, and can be shown to be relatively small in the region from 36 to 43 MeV. We have also studied the sensitivity of the predicted isomer ratio to changes in the parameters defining the statistical model. The reduction of the moment of inertia by a factor of 0.7 reduces the predicted isomer ratio by a factor of 0.8 in the plateau region. Smaller moments of inertia would be inconsistent with the value determined by the known states in ^{137}Ce with spins from $\frac{23}{2}$ to $\frac{33}{2}$.¹⁸ Changes over reasonable ranges for γ transition strengths and the level-density parameter produce changes in R of typically 10% or less.

The sensitivity of the isomer ratio to the angular momentum in the entrance channel is illustrated in Fig. 3. The results of three types of predictions are shown here, along with the experimental isomer ratios. The horizontal bars give the isomer ratio produced by decay

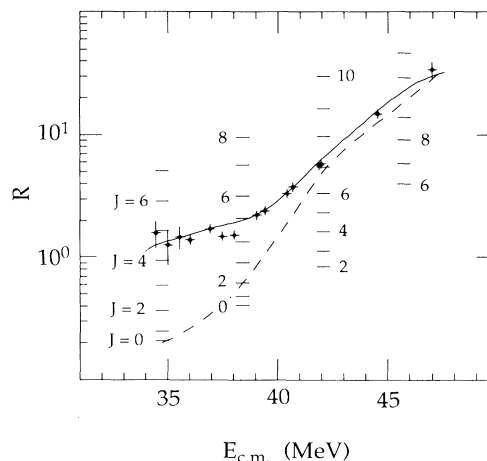


FIG. 3. The sensitivity of the calculated isomer ratio to the angular momentum in the compound nucleus. The isomer ratio is given by a unique angular momentum (horizontal bar), a sharp-cutoff distribution as described in the text (dashed curve), and the same calculation shown in Fig. 2(b) (solid curve).

of a compound nucleus having the unique indicated angular momentum. The dashed line is the isomer ratio resulting from a triangular, sharp-cutoff distribution with a total fusion cross section given by the prediction shown in Fig. 2(a). The solid curve is the same calculation shown in Fig. 2(b).

In conclusion, the measurement of the isomer ratio can be a sensitive technique for probing the average angular momentum in the entrance channel that leads to fusion. The nearly constant value for R at low energies confirms the prediction of an approximately constant value of \bar{l} at energies sufficiently far below the fusion barrier. By using a statistical model to relate the angular momentum distribution in the entrance channel to the isomer ratio (and to calculate the relative yields of the $2n$, $3n$, and $4n$ channels) we find that the energy dependence below the barrier for both $\sigma(E)$ and R is well reproduced by a barrier penetration calculation. Thus, in this energy region, the cross sections and average angular momenta are self-consistent.

We are pleased to acknowledge a number of helpful discussions with R. Vandenbosch. We thank H. Esbensen and R. Vandenbosch, respectively, for performing coupled-channel and optical-model calculations for the $^{12}\text{C} + ^{128}\text{Te}$ system. The proton-induced x-ray emission measurements were kindly made by T. Cahill. This work was supported by the Director, Office of Energy Research, Office of High Energy and Nuclear Physics, Nuclear Physics Division, of the U.S. Department of Energy under Contract No. DE-AC03-76SF00098. D.E.G. would like to thank the Consejo Nacional de Investigaciones Científicas y Técnicas for financial support.

^(a)On leave from Departamento de Fisica-TANDAR, Comisión Nacional de Energia Atómica, 1429 Buenos Aires, Argentina.

¹M. Beckerman, Phys. Rep. **129**, 145 (1985).

²W. Reisdorf, in *Proceedings of the International Nuclear Physics Conference, Harrogate, United Kingdom, August, 1986*, edited by J. L. Durell *et al.*, IOP Conference Proceedings No. 86 (Institute of Physics, Bristol and London, 1986), p. 205.

³S. Gil *et al.*, Phys. Rev. C **31**, 1752 (1985).

⁴B. Haas *et al.*, Phys. Rev. Lett. **54**, 398 (1985).

⁵T. Murakami *et al.*, Phys. Rev. C **34**, 1353 (1986).

⁶R. Vandenbosch *et al.*, Phys. Rev. Lett. **56**, 1234 (1986).

⁷C. H. Dasso and S. Landowne, Phys. Rev. C **32**, 1094 (1985).

⁸P. J. Nolan *et al.*, Phys. Rev. Lett. **54**, 2211 (1985).

⁹C. H. Dasso, H. Esbensen, and S. Landowne, Phys. Rev. Lett. **57**, 1498 (1986).

¹⁰H. Warhanek and R. Vandenbosch, J. Inorg. Nucl. Chem.

26, 669 (1964).

¹¹R. L. Kiefer and K. Street, Jr., Phys. Rev. **173**, 1202 (1968); R. L. Kiefer, Ph.D. thesis, University of California Report No. UCRL-11049, 1963 (unpublished).

¹²A. J. Pacheco *et al.*, Comput. Phys. Commun. (to be published).

¹³C. H. Dasso and S. Landowne, Phys. Lett. B **183**, 141 (1987), and Comput. Phys. Commun. **46**, 187 (1987).

¹⁴D. E. DiGregorio *et al.*, Phys. Lett. B **176**, 322 (1986).

¹⁵A. Gavron, Phys. Rev. C **21**, 230 (1980).

¹⁶D. E. DiGregorio *et al.*, Phys. Rev. C (to be published).

¹⁷R. G. Stokstad *et al.*, Phys. Rev. C **21**, 2427 (1980).

¹⁸L. K. Peker, Nucl. Data Sheets **38**, 87 (1983); M. Mueller-Veggian *et al.*, Nucl. Phys. **A304**, 1 (1978).

¹⁹A. Sierk, Phys. Rev. C **33**, 2039 (1986).

²⁰A. Gilbert and A. G. W. Cameron, Can. J. Phys. **43**, 1446 (1965).

²¹P. M. Jacobs *et al.*, Phys. Lett. B **175**, 271 (1986).